*Proc. Natl. Acad. Sci. U.S.A. 78*, 6854–6857.
Bunker, G., Stern, E. A., Blankenship, R. E., & Parson, W. W. (1982) *Biophys. J. 37*, 539–55.
Cusanovich, M. A. (1967) Ph.D. Thesis, University of California—San Diego.
Ehrenberg, A., & Kamen, M. D. (1965) *Biochim. Biophys. Acta 102*, 333–340.
Felton, R. H., & Yu, N.-T. (1978) in *The Porphyrins* (Dolphin, D., Ed.) Vol. III, pp 347–388, Academic Press, New York.
Finzel, B. C., Weber, P. C., Hardman, K. D., & Salemme, F. R. (1985) *J. Mol. Biol. 186*, 627–743.
Hoard, J. L. (1975) in *Porphyrins and Metalloporphyrins* (Smith, K. M., Ed.) p 317, Elsevier, Amsterdam.
Jameson, G. B., Molinaro, F. S., Ibers, J. A., Collman, J. P., Brauman, J. I., Rose, E., & Suslick, K. S. (1978) *J. Am. Chem. Soc. 100*, 6769–6770.
Kitagawa, T., Ozaki, Y., Kyogoku, Y., & Horio, T. (1977) *Biochim. Biophys. Acta 495*, 1–11.
Maltempo, M. M., Moss, T. H., & Cusanovich, M. A. (1974) *Biochim. Biophys. Acta 342*, 290–305.
Masuda, H., Taga, T., Osaki, K., Sugimoto, H., Yoshida, Z.-I., & Ogoshi, H. (1980) *Inorg. Chem. 19*, 950–955.
Moffat, K., Deatherage, J. F., & Seybert, D. W. (1979) *Science 206*, 1035.
Momenteau, M., Scheidt, W. R., Eigenbrot, C. W., & Reed, C. A. (1988) *J. Am. Chem. Soc. 110*, 1207–1215.
Moss, T. H., Bearden, A. J., Bartsch, R. G., & Cusanovich, M. A. (1968) *Biochemistry 7*, 1583–1596.
Powers, L. P., Chance, B., Ching, Y., & Angiolillo, P. (1981) *Biophys. J. 34*, 465–497.
Reed, C. A., Mashiko, T., Bentley, S. P., Kastner, M. E., Scheidt, W. R., Spartalian, K., & Lang, G. (1979) *J. Am. Chem. Soc. 101*, 2948–2958.
Scheidt, W. R., Geiger, D. K., Lee, Y. J., Reed, C. A., & Lang, G. (1985) *J. Am. Chem. Soc. 107*, 5693–5699.
Spiro, T. (1983) in *Iron Porphyrins* (Lever, A. P. B., & Gray, H. B., Eds.) pp 89–159, Addison-Wesley, Reading, MA.
Stern, E. A., & Heald, S. M. (1979) *Rev. Sci. Instrum. 50*, 1579.
Strekas, T. C., & Spiro, T. G. (1974) *Biochim. Biophys. Acta 351*, 237–245.
Summerville, D. A., Cohen, I. A., Hatano, K., & Scheidt, W. R. (1978) *Inorg. Chem. 17*, 2906–2910.
Tasaki, A., & Kamen, M. D. (1965) *Biochim. Biophys. Acta 140*, 284–290.
Weber, P. C., Bartsch, R. G., Cusanovich, M. A., Hamlin, R. C., Howard, A., Jordan, S. R., Kamen, M. D., Meyer, T. E., Weatherford, D. W., Xuong, Ng.-h., & Salemme, F. R. (1980) *Nature (London) 286*, 302–304.

# Determination of the Chirality of the Saturated Pyrrole in Sulfmyoglobin Using the Nuclear Overhauser Effect†

W. O. Parker, Jr., Mariann J. Chatfield, and Gerd N. La Mar*
*Department of Chemistry, University of California, Davis, California 95616*
*Received July 27, 1988; Revised Manuscript Received September 14, 1988*

ABSTRACT: The interproton nuclear Overhauser effect (NOE) and paramagnetic dipolar relaxation rates for hyperfine-shifted resonances in the proton NMR spectra of sperm whale met-cyano sulfmyoglobin have led to the location and assignment of the proton signals of the heme pocket residue isoleucine 99 (FG5) in two sulfmyoglobin isomers. Dipolar relaxation rates of these protein signals indicate a highly conserved geometry of the heme pocket upon sulfmyoglobin formation, while the similar upfield direction of dipolar shifts for this residue to that observed in native sperm whale myoglobin reflects largely retained magnetic properties. Dipolar connectivity of this protein residue to the substituents of the reacted heme pyrrole ring B defines the stereochemistry of the puckered thiolene ring found in one isomer, with the 3-$CH_3$ tilted out of the heme plane proximally. The chirality of the saturated carbons of pyrrole ring B in both the initial sulfmyoglobin product and the terminal alkaline product is consistent with a mechanism of formation in which an atom of sulfur is incorporated distally to form an episulfide across ring B, followed by reaction of the vinyl group to yield the thiolene ring that retains the $C_3$ chirality.

Recent studies on sulfmyoglobin (SMb)[1] formation based largely on NMR have provided some of the first quantitative characterization of the chemical nature of the modified green prosthetic group (Chatfield et al., 1986a–c, 1987, 1988a,b; Bondoc et al., 1987). Early optical studies had shown that the characteristic green color of SMb is likely due to a chlorin-like structure, where the insertion of an atom of sulfur into the carbon skeleton leads to saturation of a pyrrole; the addition of sulfur across the $\beta$–$\beta$ bond of hemin (**1**) to yield an episulfide, **2**, has been proposed (Berzofsky et al., 1972). $^1$H NMR studies demonstrated that SMb is generally heterogeneous, where the apparently unique initially formed species (designated $S_A$Mb) can rapidly form several major terminal equilibration products, including an alkaline product designated $S_C$Mb (Chatfield et al., 1986a,c, 1987). While $S_A$Mb possesses a prosthetic group unstable with respect to extraction (with likely structure **2**), the prosthetic group from $S_C$Mb has been extracted and its structure (Chatfield et al., 1986c), as well as that of one of its derivatives (Bondoc et al., 1986), deter-

† This research was supported by a grant from the National Institutes of Health (GM 26226).
* Address correspondence to this author.

[1] Abbreviations: SMb, sulfmyoglobin; $S_A$Mb, $S_C$Mb, isomeric forms of sulfmyoglobin; Mb, myoglobin; metMb, ferric myoglobin; NMR, nuclear magnetic resonance; ppm, parts per million; DSS, 2,2-dimethyl-2-silapentane-5-sulfonate; NOE, nuclear Overhauser effect.

0006-2960/89/0428-1517$01.50/0 

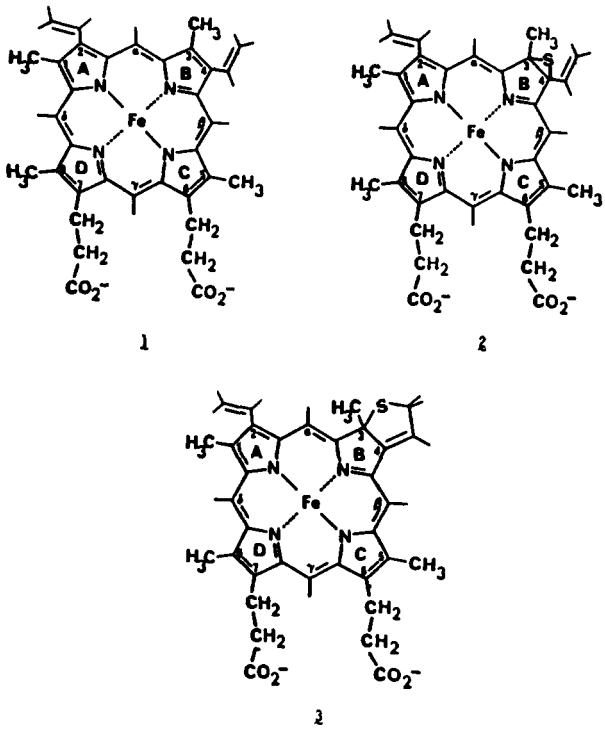

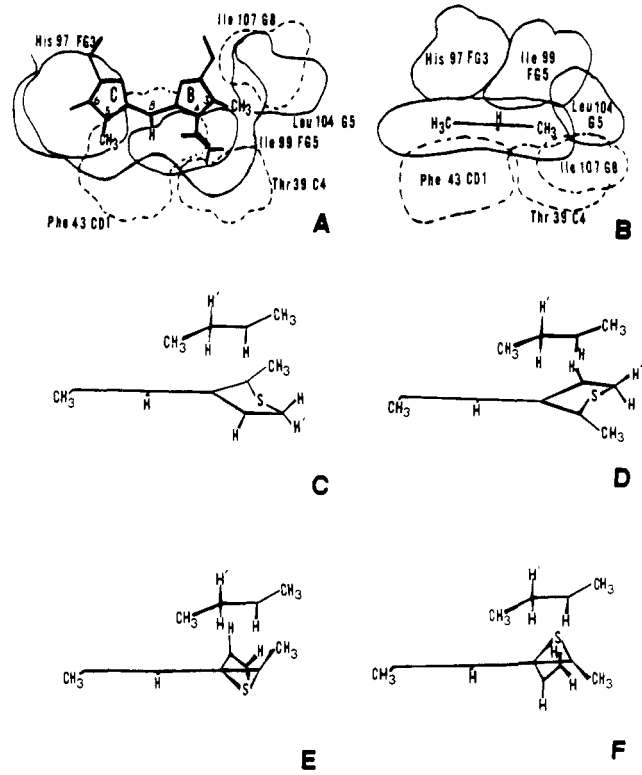

FIGURE 1: Structure and possible orientation of the substituents of pyrrole ring B of hemin and sulfhemins in sperm whale myoglobin. (A) Orientation of residues surrounding pyrrole rings B and C of hemin. The proximal side is above the plane of the page (solid lines); the distal side is below (broken lines). The β-meso-H proton is indicated by β. (B) Side-on view of (A) looking at the heme along the β–δ vector for the side of the β-meso-H. (C) Proposed orientation of pyrrole B in sulfhemin C relative to Ile 99 (FG5) formed by distal incorporation of sulfur. Note the contact of the δ-$CH_3$ to both the 5-$CH_3$ and β-meso-H of the heme, while 3-$CH_3$ and 4-$H_\beta$ contact the γ-$CH_3$. (D) Proposed orientation of pyrrole B in sulfhemin C relative to Ile 99 (FG5) formed by proximal incorporation of sulfur. (E) Proposed orientation of pyrrole in B in sulfhemin A relative to Ile 99 (FG5) formed by distal incorporation of sulfur. Note the contact of the γ-$CH_3$ to both the 5-$CH_3$ and β-meso-H of the heme, while the 3-$CH_3$ contacts the γ-$CH_3$. (F) Proposed orientation of pyrrole B in sulfhemin A relative to Ile 99 (FG5) formed via proximal incorporation of sulfur.

mined to reflect saturation of pyrrole B to yield the unusual exocyclic thiolene ring, as in **3**. Assignment of the heme vinyl and methyl signals in both high-spin and low-spin forms of the isomeric metSMbs (Chatfield et al., 1988a) as well as the extracted prosthetic group from $S_C$Mb (Chatfield et al., 1988b) has demonstrated that they each possess a saturated pyrrole B and that, at least for $S_C$Mb, the other pyrroles remain intact.

One aspect of the structure of SMbs that has not been addressed and which is a requirement for developing a detailed mechanism for the formation of $S_A$Mb is the chirality of the centers generated at $C_3$ and $C_4$. While it is likely that the activated sulfur approaches on the more open distal side, it is noted that there are "holes" in the protein on the proximal side of the heme (Takano, 1977a,b) which allow facile access to a number of divergent chemical species such as Xe (Bluhm et al., 1958; Tilton et al., 1984), $C_3H_6$ (Schoenborn et al., 1965), and $AuI_3$ and $HgI_3^-$ (Schoenborn, 1967; Kretsinger et al., 1968). Hence, attack of sulfide intercalated on the proximal side cannot be dismissed in the absence of definitive data. $^1$H NMR is particularly well suited for the determination in solution of the absolute configuration of the carbon in the saturated ring by taking advantage of the spatial selectivity of contacts with the protein matrix that can be probed by the $^1$H–$^1$H nuclear Overhauser effect (NOE) (Noggle & Shirmer, 1971). This requires first the resolution and unambiguous assignment of the proton signals of the pyrrole B substituents as well as those of the amino acid residues that make contact with both the saturated pyrrole B and an unaltered pyrrole.

$^1$H NMR spectral parameters of SMb in a number of oxidation/ligation states have indicated that the tertiary structure, particularly in the heme pocket, is largely unaltered from that of the native protein (Chatfield et al., 1987, 1988a). That the protein matrix is capable of relaxing somewhat around pyrroles A and B is witnessed by the ability to reconstitute Mb with a variety of modified hemins possessing bulky substituents on these two pyrroles (Miki et al., 1986). Thus, the general structural features of the heme cavity of the native protein are likely to apply quite well to SMbs. Moreover, detailed studies of the electronic structure of met$S_C$MbCN and the dicyano complex of its extracted prosthetic group (Chatfield et al., 1988a,b) have revealed that the orbital ground state of the iron, which determines both the contact shift and the detailed magnetic properties (Shulman et al., 1971; Byrn et al., 1983), is very similar in metSMbCN and native metMbCN. This suggests that the dipolar shift pattern (Jesson, 1973) for noncoordinated amino acid side chain groups can be expected to be qualitatively similar in the met-cyano complexes of Mb and SMb.

The chirality of the sulfhemins in $S_A$Mb or $S_C$Mb can be determined on the basis of dipolar connectivity (NOEs) between the 3-$CH_3$ and the protein matrix, as illustrated in Figure 1A,B. The relevant portion of hemin is tightly clamped between the proximal residues His 97 (FG3), Ile 99 (FG5), and Leu 104 (G4) and the distal residues Phe 43 (CD1), Thr 39 (C4), and Ile 107 (E4) (Takano, 1977a,b; Kuriyan et al., 1986), and these restraints to the two sides of the heme are unlikely to be altered in SMb. When ring B is saturated, its substituents are no longer directed along the heme plane, and 3-$CH_3$ in $S_C$Mb must point toward either the proximal (Figure 1C) or distal side (Figure 1D), depending on the chirality of $C_3$. If the sulfur atom inserts on the distal side, the stereochemistry about $C_3$ leads to $S_C$Mb and $S_A$Mb as shown in

parts C and E of Figure 1, respectively. On the other hand, insertion of the sulfur atom on the proximal side leads to an orientation of 3-$CH_3$ in $S_C$Mb and $S_A$Mb as shown in parts D and F, respectively, of Figure 1. The residue Ile 99 (FG5) satisfies the requirements of contacts with each pyrrole B and C and, in native metMbCN, exhibits the largest dipolar shifts, which place its signals well outside the intense diamagnetic envelope (Ramaprasad et al., 1983, 1984). The assignment of these signals in native metMbCN was provided by the analysis of paramagnetic relaxation and NOEs to the heme (Ramaprasad et al., 1983, 1984). Thus, for the chirality as in parts C and E in Figure 1, the close contact between the 3-$CH_3$ of pyrrole B and Ile 99 (FG5) would be maintained or possibly strengthened upon SMb formation. On the other hand, the chirality about $C_3$, as shown for $S_C$Mb in Figure 1C, would greatly increase the distance between 3-$CH_3$ and Ile 99 (FG5). An estimate of the increase in distance between 3-$CH_3$ and the closest $\delta$-$CH_3$ of Ile 99 (FG5) would be ~2.8 Å, which would yield an overall 3-$CH_3$-to-$\delta$-$CH_3$ distance of ~5–6 Å, which is larger than that for which an NOE can be reasonably detected in a paramagnetic protein.

We report herein on a study of the paramagnetic relaxation properties and NOE-detected $^1H$–$^1H$ dipolar connectivities of the environment of pyrrole B of the met-cyano form of $S_C$Mb and $S_A$Mb that establish that the chirality of the substituents about $C_3$ in each of these proteins is as shown in parts C and E of Figure 1, respectively, and confirm the largely retained magnetic properties of the iron upon formation of SMb.

## Experimental Procedures

*Sample Preparation.* The preparation of both sulfmyoglobins from sperm whale myoglobin (Sigma) has been previously described in detail (Chatfield et al., 1987). Proteins were 3 mM in 500 μL of 0.1 M phosphate buffer, pH 8.1, in $^2H_2O$. The pH was measured with a Beckman 3550 pH meter equipped with an Ingold 620 microcombination electrode; pH values are uncorrected for isotope effect.

*Data Collection.* $^1H$ NMR spectra were recorded on a Nicolet NT-360 FTNMR spectrometer operating at 360 MHz in the quadrature mode. Optimal resolution of the signals of interest was obtained at 40 °C, but lower temperatures were used for NOE studies to minimize degradation of the samples (25 °C for $S_A$Mb, 30 °C for $S_C$Mb). Data were collected by using double precision on 16 384 data points over a 50-kHz bandwidth. Chemical shifts are referenced to 2,2-dimethyl-2-silapentane-5-sulfonate (DSS) through the residual water resonance. Resolution enhancement of reference spectra (Figures 3A–E, 5A, 6A, and 7A) was performed via apodization of the free induction decay using double-exponential multiplication, which was followed by zero-filling to 32 768 points prior to Fourier transformation. Because this type of deconvolution slightly alters the relative intensity of broad peaks, these spectra were used only to locate peaks and not to quantitate them. Peaks of residual myoglobin and other sulfmyoglobin products were identified by observation of independently prepared samples containing various amounts of the impurity proteins (Figure 3).

Nuclear Overhauser spectra were recorded by application of a presaturation pulse of 80 ms with the decoupler on-resonance. Corresponding reference spectra were collected under identical conditions but with the decoupler pulse off-resonance. On- and off-resonance frequencies were alternated every 128 scans. Typical spectra consisted of at least 5000 transients collected with a repetition rate of 0.2 $s^{-1}$. Off-resonance effects were eliminated, when possible, by placing the reference frequency symmetrically about the undesired resonance from that of the irradiated signal. When this was not practical, off-resonance effects were distinguished from NOEs by observation at two different power levels at which NOEs were retained but spillage effects were increased or decreased according to the power used. Such effects are noted in the figures.

$T_1$ measurements were performed by using the inversion-recovery method with composite inversion pulses (Levitt & Freeman, 1979; Levitt, 1982) and phase alteration (Cutnell et al., 1976); delays between scans were maintained to be $>5T_1$. $T_1$s were obtained from standard semilogarithmic plots, with errors of ±10%; $T_1$s of partially resolved resonances were taken from the null point, $\tau_{null}$, via $\tau_{null}/\ln 2$, with uncertainties of ±20%.

All preparations of sulfmyoglobins contain at least 5% native myoglobin, as well as minor impurities, and various forms of SMb are often generated during the time required for NOE observation (Chatfield et al., 1987). To account for these products, all observations were carried out on at least two independently prepared samples containing differing amounts of side products (Figure 3) and the results compared accordingly. To aid in analysis, measurements on partially resolved resonances were also recorded at two different temperatures. NOEs from underlying resonances of side products or myoglobin (Ramaprasad et al., 1983, 1984) and other peaks of those products are accounted for in the figures.

*Data Analysis.* The magnitude of the steady-state nuclear Overhauser effect relationship is given by (Noggle & Shirmer, 1971)

$$\eta_{ij} = \sigma_{ij}/\rho_j \quad (1)$$

where $\eta_{ij}$ is the fractional intensity change for the signal of spin $j$ while saturating spin $i$, $\sigma_{ij}$ is the cross-relaxation rate between spins $i$ and $j$, and $\rho_j$ is the intrinsic relaxation rate for spin $j$. For a pair of protons separated by a distance $r_{ij}$, the cross-relaxation rate in the applicable slow-motion limit is given by (Noggle & Shirmer, 1971)

$$\sigma_{ij} = -h^2\gamma^4\tau_c/10r_{ij}^6 \quad (2)$$

where $\tau_c$ is the reorientation time of the $i$–$j$ vector, taken to be 7 ns in myoglobin at 30 °C (La Mar et al., 1986). Thus, if $\eta_{ij}$ and $\rho_j$ are known, $\sigma_{ij}$ can be solved for $r_{ij}$.

The intrinsic relaxation rate of spin $j$ is the sum of diamagnetic and paramagnetic terms (Swift, 1973):

$$\rho_j = \rho_{dia} + \rho_{para} \quad (3)$$

However, spin–lattice relaxation via diamagnetic mechanisms is, for the most part, ineffective, and for very fast relaxing spins, as seen in the sulfglobins, the $\rho_{para}$ term must dominate. Under these conditions

$$\rho_j \cong \rho_{para} = T_1^{-1} = (AR^{-6} + B\rho^2)T_{1e} \quad (4)$$

where $R$ is the distance from the metal, $\rho$ is the $\pi$ spin density at the adjacent pyrrole carbon, $T_{1e}$ is the electron spin–lattice relaxation time, and $A$ and $B$ are constants for a given system of interest (Unger et al., 1985). If the second term approaches zero, as for amino acids ($\rho^2 = 0$) and for meso substituents ($B\rho^2 \rightarrow 0$), or if it is corrected for contact contributions as in Figure 3 (see text), then (Swift, 1973)

$$T_{1j}^{-1}/T_{1i}^{-1} = R_j^{-6}/R_i^{-6} \quad (5)$$

Thus, determination of the $T_1$ ratio for two peaks for which $R_j$ is known leads directly to $R_i$.

## Results and Discussion

The very similar orbital ground state of the iron in both SMb and native Mb met-cyano complexes (Chatfield et al.,

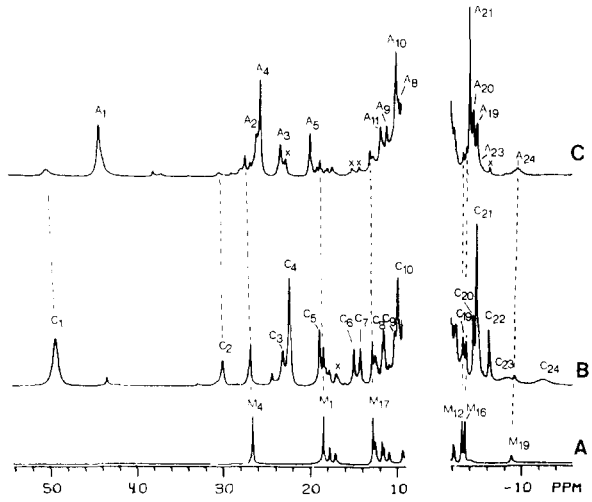


FIGURE 2: 360-MHz $^1H$ NMR spectra in $^2H_2O$ of the complexes of (A) metMbCN, pH 7.6, at 30 °C, (B) met$S_C$MbCN, pH 7.8, at 30 °C, and (C) met$S_A$MbCN, pH 8.1, at 25 °C. The slight difference in chemical shifts between samples is due to a pH effect. $M_i$, $C_i$, and $A_i$ designate resonances of metMbCN, met$S_C$MbCN, and met$S_A$MbCN, respectively. Assignments are summarized in Table I. Impurities and other sulfmyoglobin products are labeled ×.

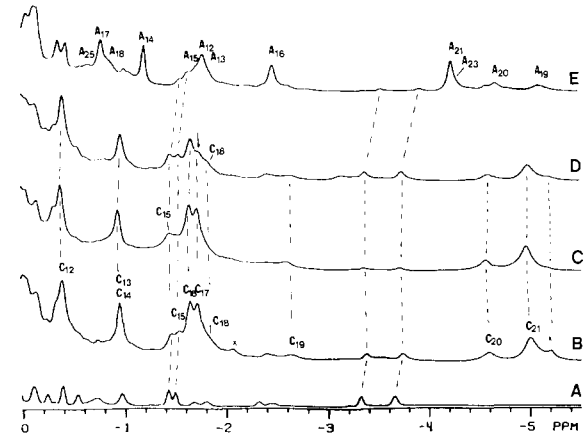


FIGURE 3: Expanded regions of the 360-MHz $^1H$ NMR spectra of sulfmyoglobin. (A) MetMbCN, pH 7.6, at 30 °C. (B) Met$S_C$MbCN, pH 7.8, at 30 °C, with 15% metMbCN and 10% impurities (×). (C) Met$S_C$MbCN, pH 8.1, 30 °C, with 5% metMbCN and <5% impurities. The sample is perdeuteriated at the hemin meso-Hs, which does not affect this spectral region (Chatfield et al., 1988a). The increased purity in this sample, however, allows clear observation of otherwise obscured met$S_C$MbCN resonances such as $C_{15}$. (D) Met$S_C$MbCN, pH 8.0, 30 °C. This sample is deuterium-labeled at the 8-$CH_3$ (65%) (Chatfield et al., 1988a), allowing observation of the broad resonance $C_{18}$, which is partially obscured by the 8-$CH_3$ resonance in trace B. (E) Met$S_A$MbCN, pH 8.0, at 25 °C. Resonances of metMbCN, met$S_C$MbCN, and met$S_A$MbCN are labeled $M_i$, $C_i$, and $A_i$, respectively; impurities are designated ×. Spectra are resolution-enhanced via double-exponential multiplication as described under Experimental Procedures, causing slight alteration of relative peak intensities.

1988b) leads to the expectation of similar magnetic properties (Shulman et al., 1971; Byrn et al., 1983), which suggests dipolar shifts of the same direction in met-cyano complexes of both native and sulfmyoglobin, but not necessarily of the same magnitude. The residue of interest that has contact with both pyrroles B and C, Ile 99 (FG5), experiences the strongest upfield dipolar shift in metMbCN (Ramaprasad et al., 1983, 1984; Lecomte et al., 1985), but the reduced anisotropy of met-cyano SMb, as witnessed by a smaller spread in $g$ values (Berzofsky et al., 1971), suggests that the dipolar shifts can be expected to be smaller in the SMb complexes. The initial focus of this paper will be to locate and assign unambiguously these Ile 99 (FG5) resonances in both met$S_A$MbCN and met$S_C$MbCN and then to determine their proximity to the necessarily out-of-heme plane 3-$CH_3$. Other assignments are not pursued at this time except as they are found necessary to establish the stereochemistry of pyrrole B in the heme cavity.

*Spectral Analysis.* The complete spectra of met$S_C$MbCN and met$S_A$MbCN are illustrated in parts B and C of Figure 2, respectively, where they are also compared to that of native metMbCN (trace A). The crowded upfield region of interest is expanded in Figure 3; the amount of native metMbCN is variable from 5 to 15% but can be readily identified by comparison to the trace in (A). Isotope-labeling experiments (Chatfield et al., 1986c, 1988a) had previously identified the resolved met$S_C$MbCN resonances $C_1$ (1-$CH_3$), $C_4$ (5-$CH_3$), $C_5$ (2-$H_\alpha$), $C_6$,$C_7$ (4-$H_\beta$s), $C_8$,$C_9$ (two meso-Hs), $C_{17}$ (8-$CH_3$), $C_{21}$ (3-$CH_3$), and $C_{22}$ (4-$H_\alpha$) and the met$S_A$MbCN peaks $A_1$ (1-$CH_3$), $A_4$ (5-$CH_3$), $A_5$ (2-$H_\alpha$), $A_8$,$A_9$ (two meso-Hs), $A_{17}$ (8-$CH_3$), and $A_{21}$ (3-$CH_3$). Only the two propionate $\alpha$-$CH_2$ were not labeled, although $C_2$,$C_3$ and $A_2$,$A_3$ can be tentatively attributed to 6-$\alpha$-$CH_2$ on the basis of their resemblance in unique shift to that of the strikingly similar spectrum of the extracted dicyanosulfhemin C (Chatfield et al., 1988b), for which a complete assignment could be effected on the basis of multiplet structure and relaxation properties.

The crowded upfield region shown in Figure 3B contains numerous composite resonances whose relative intensities can be ascertained from a combination of pH and variable-temperature studies. Peaks that track with three-proton intensity under all circumstances are assigned as methyls. For met$S_C$MbCN, such methyl peaks are $C_{12}$, $C_{14}$ (which resolves from $C_{13}$ at 35 °C; not shown), and $C_{16}$. Upon deuteriation of 8-$CH_3$ ($C_{17}$, Figure 3D), its broad upfield shoulder ($C_{18}$) has intensity suggestive of a methyl peak, but which could not be quantified. Prominent narrow single-proton peaks are the resolved $C_{19}$ and $C_{20}$, $C_{15}$ [which is overlapped by intense residual metMbCN peaks; a sample of mesodeuteriated met$S_C$MbCN (trace C) that contains much less native metMbCN allows its detection more clearly], and $C_{13}$ (resolved at 35 °C, not shown). The upfield region of met$S_A$MbCN (Figure 3E) exhibits three unassigned apparent methyl peaks, $A_{12}$, $A_{14}$, and $A_{16}$, as well as a broad peak ($A_{18}$), which also could arise from a methyl. The unassigned single-proton peaks are $A_{15}$, $A_{19}$, $A_{20}$, and $A_{25}$ (see below), as well as apparent $A_{13}$ on the high-field shoulder of $A_{12}$.

*Relaxation Times.* Nonselective $T_1$s for all resolved or partially resolved peaks for both met$S_A$MbCN and met$S_C$MbCN were obtained by the inversion-recovery technique, and the values are listed in Table I. It is observed that the $T_1$s of the resolved and assigned heme methyls vary significantly. Since the heme methyls are essentially equidistant from the iron, this dictates that, in addition to the metal-centered relaxation, there are important contributions from dipolar relaxation through delocalized spin density, as seen in model complexes (Unger et al., 1985; Chatfield et al., 1988b) and native metMbCN (Cutnell et al., 1981) and given by the relation of eq 4.

A measure of the contribution from the metal-centered relaxation ($AR^{-6}T_{1e}$) to a methyl can be obtained from the intercept of a straight line plot of observed $T_{1H}^{-1}$ versus the square of observed contact shift ($\propto \rho^2$), as discussed in detail elsewhere (Unger et al., 1985). Such plots for metMbCN, met$S_C$MbCN, and met$S_A$MbCN are given in Figure 4. The straight lines through the data points for each of the three complexes are approximately parallel and predict approximate ratios of metal-centered dipolar relaxation rates ($AR^{-6}T_{1e}$) of

Table I: Assignment of Resonances Relevant to Determination of the Conformation and Chirality of Ring B in the Sulfmyoglobin Isomers, pH 8

| heme peaks | | metS$_A$MbCN, 25 °C | | | metS$_C$MbCN, 30 °C | | | metMbCN, 25 °C | |
|---|---|---|---|---|---|---|---|---|---|
| $\chi_i$[a] | assignment[b] | shift[c] | $T_1$ (ms) | intercept[d] | shift[c] | $T_1$ (ms) | intercept[d] | shift[c] | $T_1$ (ms) |
| 1 | 1-$CH_3$ | 44.00 | 25 | −3.9 | 49.10 | 19 | −1.9 | 18.29 | 123 |
| 4 | 5-$CH_3$ | 25.48 | 30 | 1.0 | 22.19 | 24 | 0.2 | 26.43 | 94 |
| 5 | 2-$H_\alpha$ | 19.75 | 30 | 8.4 | 18.75 | 26 | 5.7 | 17.58 | 108 |
| 6 | 4-$H_\beta'$ | *e* | *e* | *e* | 14.77 | 47 | 3.5 | – | – |
| 7 | 4-$H_\beta$ | *e* | *e* | *e* | 14.06 | 41 | 9.0 | – | – |
| 8 | $\beta$-meso-H | 9.61 | 14 | 10.0 | 11.38 | 11 | 10.1 | – | – |
| 17 | 8-$CH_3$ | −0.77 | 70 | 5.8 | −1.71 | 52 | 3.7 | 12.62 | 154 |
| 21 | 3-$CH_3$ | −4.24 | 55 | 2.6 | −5.01 | 29 | 0.7 | – | – |
| 22 | 4-$H_\alpha$ | *e* | *e* | *e* | −6.36 | 32 | 4.8 | – | – |
| Ile 99 (FG5) | | metS$_A$MbCN, 25 °C | | | metS$_C$MbCN, 30 °C | | | metMbCN, 25 °C | |
| $\chi_i$[a] | assignment[b] | shift[c] | $T_1$ (ms) | intercept[d] | shift[c] | $T_1$ (ms) | intercept[d] | shift[c] | $T_1$ (ms) |
| 12 | $\delta$-$CH_3$ | −1.76 | 60 | 0.5 | −0.39 | *e* | 0.2 | −3.66 | 188 |
| 13 | $\alpha$-CH[f] | −1.76 | *e* | *e* | −0.97 | *e* | 3.2 | −2.2 | |
| 16 | $\gamma$-$CH_3$ | −2.47 | 70 | 2.6 | −1.66 | 63 | 0.9 | −3.32 | 199 |
| 19 | $\gamma$-CH′ | −5.10 | 15 | 7.9 | −2.65 | 14 | 7.0 | −9.05 | 65 |
| 25 | $\gamma$-CH | −0.67 | *e* | *e* | 0.26 | *e* | *e* | −1.69 | *e* |
| 26 | $\beta$-CH[f] | 0.05 | *e* | *e* | 0.02 | *e* | *e* | 0.03 | *e* |

[a] As in structures **1–3** and as $M_i$, $A_i$, and $C_i$ in Figure 1. [b] Assignments and relaxation data for myoglobin from Ramaprasad et al. (1984); those of sulfmyoglobins from Chatfield et al. (1988a) and in text. [c] Chemical shift in ppm from DSS. [d] Intercept in a Curie plot at $T^{-1} = 0$. [e] Not resolved or determined. [f] Tentative assignment.

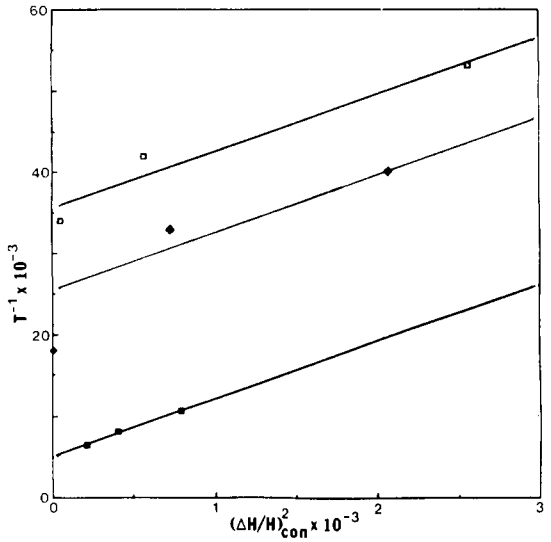


FIGURE 4: Plot of observed $T_1^{-1}$ versus $[(\Delta H/H)_{con}]^2$ for resolved methyl groups of the met-cyano complexes of metMbCN (solid squares, bottom line), metS$_C$MbCN (open squares, top line), and metS$_A$MbCN (solid diamonds, middle line). Solid lines describe the best fit to the expected straight line. The intercept at $[(\Delta H/H)_{con}]^2 = 0$ gives the solely metal-centered dipolar contribution to the relaxation rate of heme methyls (Unger et al., 1985; Chatfield et al., 1988b).

~6:~4:1 for metS$_C$MbCN:metS$_A$MbCN:metMbCN. Since *A* and *R* are identical for the three complexes, this ratio must also hold for their relative $T_{1e}$ values. Hence, similarly positioned noncoordinated amino acid protons should exhibit this same ratio of relaxation rates in the three proteins. A qualitative test of this is the ratio of $T_1$s for meso-H peaks in metS$_A$MbCN (~15 ms) and metS$_C$MbCN (10 ms), ~1.5, which is the same as obtained from the relative intercepts in Figure 4; the meso-H peaks are not resolved in native metMbCN, and hence the $T_1$s are unknown.

Thus, on the basis of the known close distance of Ile 99 (FG5) to the iron [4.5 Å for $\gamma$-CH (Takano, 1977)] and its short $T_1$ [~50 ms (Ramaprasad et al., 1984)] in metMbCN, we expect the analogous Ile 99 (FG5) proton to have much shorter $T_1$s, in the range of 15 and 10 ms for metS$_A$MbCN and metS$_C$MbCN, respectively. Of the relatively narrow resolved single protons in the upfield window, $A_{19}$ and $C_{19}$ exhibit the shortest $T_1$s, 15 and 14 ms, respectively. These $T_1$s are very similar to those of meso-Hs in the same complex, which confirms the ~4.5-Å distance from the iron via eq 5 since meso-H exhibits negligible contact shift (i.e., $\rho^2 \sim 0$ in eq 4).

*Pyrrole B Conformation.* The saturation of pyrrole B in S$_C$Mb forms a thiolene ring structure that must be strongly puckered. Maintaining maximal coplanarity for the remaining three pyrroles leads to one 4-$H_\beta$ (designated 4-$H_\beta'$) being more in-plane with the 4-$H_\alpha$ [as witnessed by differential $J(H_\alpha$–$H_\beta)$ in the dicyano complex of the extracted group (Chatfield et al., 1986c)] and the other 4-$H_\beta$ closer to the out-of-plane 3-$CH_3$ (Figure 1C,D). These modified pyrrole substituents exhibit resolved resonances that allow determination of their stereochemistry.

Saturation of 3-$CH_3$ ($C_{21}$) (Figure 5B) yields an NOE to only one 4-$H_\beta$,$C_7$, dictating that $C_7$ is 4-$H_\beta$ rather than 4-$H_\beta'$ in part C or D of Figure 1, as well as an NOE to the methyl peak $C_{16}$. Upon saturating 4-$H_\beta$ ($C_7$), we observe the reciprocal NOE to 3-$CH_3$ ($C_{21}$), a small NOE to 4-$H_\alpha$ ($C_{22}$), and a large NOE to its known geminal partner, 4-$H_\beta'$ ($C_6$) (Figure 5C). The large NOEs in the diamagnetic envelope 1–4 ppm must arise from an unidentified amino acid.[2] When 4-$H_\beta'$ is saturated (Figure 5D), the reciprocal large NOE to $C_7$ is seen, as well as one to 4-$H_\alpha$ but not to 3-$CH_3$; the same two amino acid peaks[2] are also observed as in Figure 5C. Saturation of 4-$H_\alpha$ ($C_{22}$) exhibits a factor ~2 larger NOE to 4-$H^{\beta'}$ ($C_6$) than to 4-$H_\beta$ ($C_7$), as well as an NOE to methyl peak $C_{12}$ (Figure 5E). The larger NOE from the 4-$H_\beta'$ ($C_6$) than from the 4-$H_\beta$ ($C_7$) to 4-$H_\alpha$ ($C_{22}$), the much larger NOE from 4-$H_\beta$ ($C_7$) than from the 4-$H_\beta'$ ($C_6$) to the 3-$CH_3$ ($C_{21}$), and the larger NOE from 4-$H_\alpha$ ($C_{22}$) to 4-$H_\beta'$ ($C_6$) than from the 4-$H_\beta$ ($C_7$) confirm the expected pucker of the thiolene ring as shown in Figure 1C,D.

Since the 4-vinyl peaks for metS$_A$MbCN are not resolved, the relative spatial configurations of the pyrrole B substituents could not be determined at this time.

*Assignment of Ile 99 (FG5).* Upon saturating the rapidly relaxing proton signal $C_{19}$ in metS$_C$MbCN (Figure 6B), we observe solely NOEs to the two upfield methyl signals $C_{12}$ and

[2] The size of the NOE to these unassigned resonances indicates a very close contact to a neighboring amino acid, most likely Thr 39 (C4), which is partially in the heme plane near the 4-vinyl in native Mb.

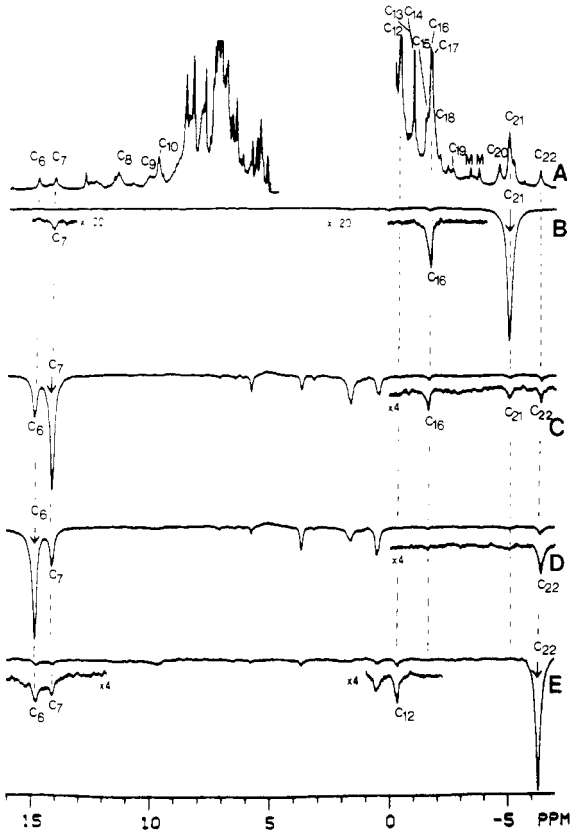


FIGURE 5: (A) 360-MHz $^1H$ NMR reference spectrum of met$S_C$MbCN in $^2H_2O$, pH 7.8, 30 °C, relevant to determination of the stereochemistry of pyrrole ring B substituents. Previously assigned heme resonances are $C_6$(4-$H_\beta'$), $C_7$(4-$H_\beta$), $C_{21}$(3-$CH_3$), and $C_{22}$(4-$H_\alpha$) (Chatfield et al., 1986c, 1988a); peak designations are those of Figures 2 and 3. The spectrum has been resolution-enhanced via application of double-exponential multiplication to the data prior to Fourier transformation to clarify individual resonances (see Experimental Procedures). (B–E) Difference spectra generated by subtracting the reference spectrum of A (non-resolution-enhanced) from a similar spectrum of the same sample in which one of the resonances was presaturated (saturated signals are indicated by arrows). (B) Saturate $C_{21}$ (3-$CH_3$); note the NOE to $C_7$ (4-$H_\beta$) and $C_{16}$ (Ile 99 (FG5) $\gamma$-$CH_3$). (C) Saturate $C_7$ (4-$H_\beta$); note the NOE to $C_6$ (4-$H_\beta'$), $C_{21}$ (3-$CH_3$), and $C_{22}$ (4-$H_\alpha$) as well as to $C_{16}$ [Ile 99 (FG5) $\gamma$-$CH_3$]. (D) Saturate $C_6$ (4-$H_\beta'$); note the NOE to $C_7$ (4-$H_\beta$) and $C_{22}$ (4-$H_\alpha$). (E) Saturate $C_{22}$ (4-$H_\alpha$); note the NOE to $C_6$ (4-$H_\beta'$) and $C_7$ (4-$H_\beta$) as well as to $C_{12}$ [Ile 99 (FG5) $\delta$-$CH_3$].

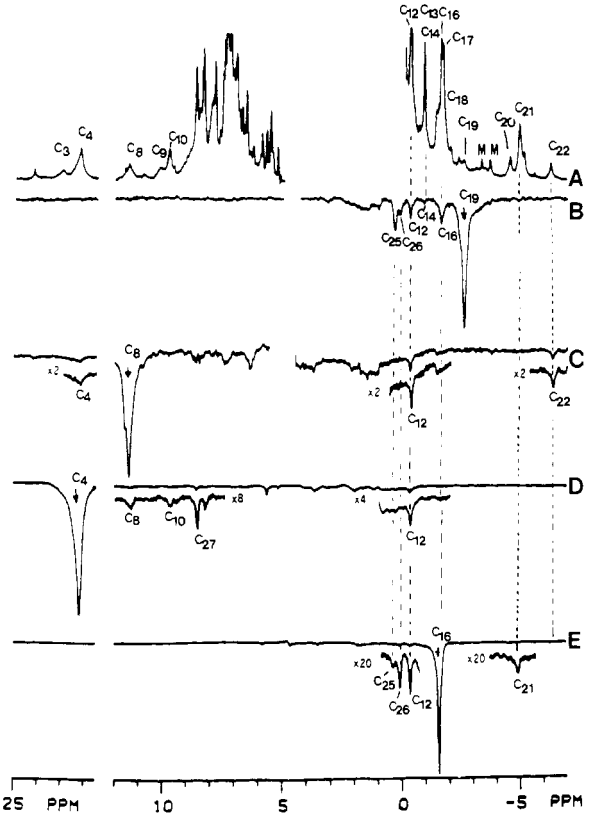


FIGURE 6: (A) 360-MHz $^1H$ NMR resolution-enhanced reference spectrum of met$S_C$MbCN in $^2H_2O$, pH 7.8, 30 °C, relevant to assignment of Ile 99 (FG5) resonances, with peak designations of Figures 2 and 3. Previously assigned resonances are $C_4$ (5-$CH_3$), $C_8$ (meso-H), $C_{21}$ (3-$CH_3$), and $C_{22}$ (4-$H_\alpha$) (Chatfield et al., 1986c, 1988a). (B–E) Difference spectra for the sample described in (A) generated as explained in Figure 5; arrows designate irradiated peaks. (B) Saturate $C_{19}$ [$\gamma$-CH of Ile 99 (FG5)]; note NOE to Ile 99 (FG5) resonances $C_{25}$ ($\gamma$-CH′), $C_{26}$ ($\beta$-CH), $C_{12}$ ($\delta$-$CH_3$), $C_{14}$ ($\alpha$-CH), and $C_{16}$ ($\gamma$-$CH_3$). (C) Saturate $C_8$ ($\beta$-meso-H); note NOE to $C_4$ (5-$CH_3$) and $C_{22}$ (4-$H_\alpha$) as well as to $C_{12}$ ($\delta$-$CH_3$). (D) Saturate $C_4$ (5-$CH_3$); note NOE to $C_8$ ($\beta$-meso-H) and $C_{12}$ [$\delta$-$CH_3$ of Ile 99 (FG5)]. (E) Saturate $C_{16}$ [$\gamma$-$CH_3$, Ile 99 (FG5)]; note NOE to $C_{21}$ (3-$CH_3$) and the Ile 99 (FG5) resonances $C_{25}$ ($\gamma$-CH′), $C_{26}$ ($\beta$-CH), and $C_{16}$ ($\gamma$-$CH_3$).

$C_{16}$, as well as to two unresolved signals designated $C_{25}$ and $C_{26}$. The NOE to $C_{25}$ is ~20%, which is too large to be to another methyl, and hence is most likely to arise from a NOE to a single proton geminal partner (Ramaprasad et al., 1984). This pattern of four NOEs from an upfield efficiently relaxed non-heme single proton is reminiscent of the pattern observed for $\gamma$-CH of the desired Ile 99 (FG5) residue in native metMbCN (Ramaprasad et al., 1983, 1984). The identity of $C_{25}$ as a single proton, and hence as a geminal partner to $C_{19}$, is supported by similar data for met$S_A$MbCN (see below), for which the analogous peak to $C_{25}$ can be established as a single proton. The NOEs among the peaks $C_{19}$, $C_{12}$, $C_{16}$, $C_{25}$, and $C_{26}$ are consistent with an Ile or a Leu, and the short $T_1$ for $C_{19}$ places at least one proton of the residue at only ~4.5 Å from the iron. The three Leu/Ile residues in the heme pocket are Ile 99 (FG5), Ile 107 (G8), and Leu 104 (G5), all of which have close contact with 3-$CH_3$ in native metMbCN (Takano, 1977a,b). However, as shown in Figure 1A,B, only Ile 99 (FG5) is close to substituents on both pyrroles B and C. Both Ile 107 and Leu 104 make contact solely with pyrroles A and B (Figure 1A,B). Moreover, the closest single protons of Ile 107 and Leu 104 are 6.2 and 6.1 Å (Takano, 1977a,b), respectively, while the proton giving rise to $C_{19}$ (or $A_{19}$) is found only ~4.5 Å from the iron (see above).

Saturation of the previously identified (Chatfield et al., 1988a) meso-H peak $C_8$ (Figure 6C) yields NOEs to both 5-$CH_3$ ($C_4$) and 4-$H_\alpha$ ($C_{26}$), identifying it clearly as the $\beta$-meso-H. Moreover, $C_8$ also yields an NOE to $C_{12}$, the methyl associated with the same amino acid containing $C_{16}$, $C_{19}$, $C_{25}$, and $C_{26}$. Irradiation of 5-$CH_3$ ($C_4$) gives the reciprocal small NOE to $C_8$ ($\beta$-meso-H) as well as a significant NOE to the same $C_{12}$ (Figure 6D). The proximity of methyl peak $C_{12}$ to both 5-$CH_3$ and $\beta$-meso-H establishes that Ile 99 (FG5) must give rise to peaks $C_{12}$, $C_{16}$, $C_{19}$, $C_{25}$, and $C_{26}$ and moreover dictates that $C_{12}$ is $\delta$-$CH_3$, $C_{16}$ is $\gamma$-$CH_3$ $C_{19}$ is $\gamma$-CH, and $C_{25}$ is $\gamma$-CH′, with $C_{26}$ probably $\beta$-CH (Figure 1C,D). When $C_{16}$ ($\gamma$-$CH_3$) is saturated (Figure 6E), we clearly see that NOE to 3-$CH_3$ ($C_{21}$), just as saturation of 3-$CH_3$ above (Figure 5B) revealed a strong NOE from 3-$CH_3$ to $C_{16}$ ($\gamma$-$CH_3$). The dipolar connectivity among Ile 99 (FG5) protons and between these and the 5-$CH_3$ and 3-$CH_3$ are the same as have been observed in native metMbCN (Ramaprasad et al., 1984; Lecomte et al., 1985; La Mar et al., 1986).

The data in Figure 7 allow us to effect an assignment of Ile 99 (FG5) signals of met$S_A$MbCN along similar lines. Saturation of the rapidly relaxing non-heme single-proton peak

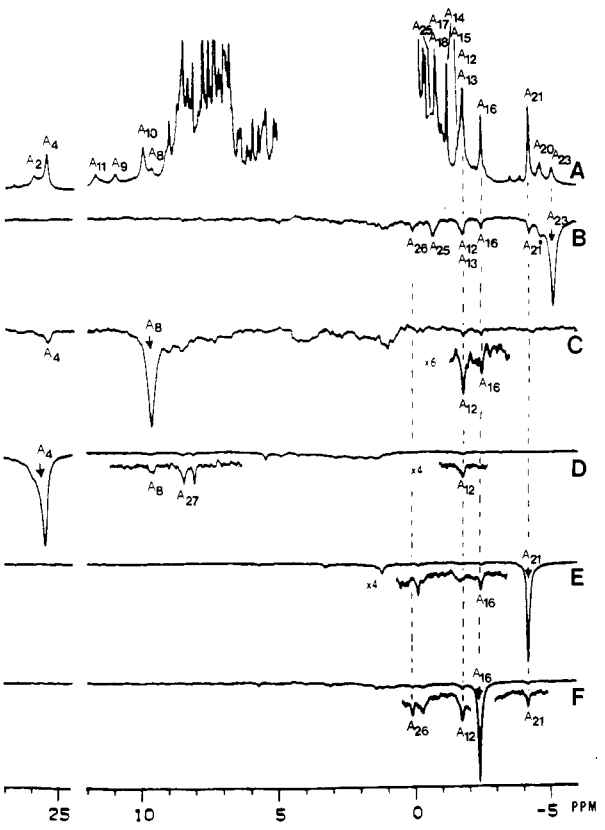


FIGURE 7: (A) 360-MHz $^1H$ NMR reference spectrum of met-$S_A$MbCN in $^2H_2O$, pH 8.1, 25 °C, relevant to the assignment of Ile 99 (FG5) resonances. Labeling is that of Figures 2 and 3; arrows designate irradiated peaks. Previously assigned resonances (Chatfield et al., 1988a) are $A_4$ (5-$CH_3$), $A_8$ (meso-H), and $A_{21}$ (3-$CH_3$). This spectrum has been resolution-enhanced, as described under Experimental Procedures. (B–F) Difference spectra for the sample described in (A) generated as explained in Figure 5. Black dots indicate decoupler spillage to neighboring resonances. (B) Saturate $A_{23}$ [$\gamma$-CH of Ile 99 (FG5)]. Note NOE to Ile 99 (FG5) resonances $A_{26}$ ($\beta$-CH), $A_{25}$ ($\gamma$-CH′), $A_{12}$ ($\delta$-$CH_3$), $A_{13}$ ($\alpha$-CH), and $A_{16}$ ($\gamma$-$CH_3$) as well as to $A_{21}$ (3-$CH_3$). The NOE to $A_{13}$ occurs under $A_{12}$, but can be distinguished at 20 °C (not shown). (C) Saturate $A_8$ ($\beta$-meso-H); note NOE to $A_4$ (5-$CH_3$) and to Ile 99 (FG5) peaks $A_{12}$ ($\delta$-$CH_3$) and $A_{16}$ ($\gamma$-$CH_3$). (D) Saturate $A_4$ (5-$CH_3$); note NOE to $A_8$ ($\beta$-meso-H) and $A_{12}$ [$\delta$-$CH_3$ of Ile 99 (FG5)]. (E) Saturate $A_{21}$ (3-$CH_3$); note NOE to $A_{16}$ [$\gamma$-$CH_3$ of Ile 99 (FG5)]. (F) Saturate $A_{16}$ ($\gamma$-$CH_3$); note NOE to $A_{21}$ (3-$CH_3$), $A_{26}$ ($\beta$-CH), and $A_{12}$ ($\delta$-$CH_3$).

$A_{19}$ (Figure 7B) yields a large NOE to $A_{25}$ (~20%), as well as NOEs to methyl non-heme peaks $A_{12}$ and $A_{16}$ and a small NOE to a nonresolved peak designated $A_{26}$. In this case the line width of $A_{25}$ in the NOE difference trace (Figure 7B) together with the intensity of that peak in the reference trace dictates that $A_{25}$ must be a single-proton peak, and hence its large NOE must be due to $A_{25}$ being a geminal partner to $A_{19}$ (Ramaprasad et al., 1984). Thus, the pattern of NOEs from $A_{19}$ is very similar to that observed for $C_{19}$ (Figure 6B) as well as to that for $\gamma$-CH of Ile 99 in native metMbCN (Ramaprasad et al., 1983, 1984).

Saturation of the previously located meso-H peak $A_8$ (Chatfield et al., 1988a) gives rise to NOEs to 5-$CH_3$ ($A_4$) as well as small NOEs to $A_{12}$ and $A_{16}$ and hence identifies $A_8$ as $\beta$-meso-H (Figure 7C). Saturating 5-$CH_3$ ($A_4$) gives a small reciprocal NOE to $A_8$ as well as an NOE to $A_{12}$, $A_{20}$ (Figure 7D).[3] Irradiation of 3-$CH_3$ ($A_{21}$) yields an NOE to $A_{16}$ (Figure 7E),[4] while saturation of $A_{16}$ leads to NOEs to both $A_{19}$ and 3-$CH_3$ ($A_{21}$) (Figure 7F). This locates the residue over pyrroles B and C and identifies $A_{12}$ and $A_{16}$ as the $\delta$-$CH_3$ and $\gamma$-$CH_3$, respectively, and $A_{19}$ and $A_{25}$ as $\gamma$-CH and $\gamma$-CH′, respectively, on Ile 99 (FG5).

The chemical shifts for both the known heme and the presently determined Ile 99 (FG5) resonances, together with the variable-temperature intercepts at $T^{-1} \cong 0$, are included with the $T_1$ data in Table I.

It may be noted that the relative relaxation rates ($T_1^{-1}$s) for the Ile 99 $\gamma$-CH, $\gamma$-$CH_3$, and $\delta$-$CH_3$ and the metal-centered contribution to a heme methyl (i.e., intercept in Figure 3) are 2.2:0.5:$C_{16}$[4]:1.0 and 3.3:0.7:0.9:1.0 for met$S_C$MbCN and met$S_A$MbCN, respectively, which are very similar to the ratio previously reported for metMbCN, namely, 2.5:0.9:0.9:1.0 (Ramaprasad et al., 1984). In particular, the very similar ratio of $T_1^{-1}$ ($\gamma$-CH):$T^{-1}$ (heme methyl) dictates that the Ile 99 has not significantly altered its orientation upon SMb formation. Moreover, the ratios of $T_1^{-1}$ ($\gamma$-$CH_3$), 4.6:4.3:1.0 for met$S_C$MbCN:met$S_A$MbCN:metMbCN, are similar to that determined for the metal-centered contribution in the heme methyls, as shown in Figure 4.

*Chirality about $C_3$.* The distance between $\gamma$-$CH_3$ of Ile 99 (FG5) and the heme 3-$CH_3$ is 3.8 ± 0.1 Å in the X-ray crystal structues of met$MbH_2O$ and MbCO (Takano, 1977a; Kuriyan et al., 1986). If the chirality about $C_3$ was as shown in part D of Figure 1, where the sulfur alone was inserted on the proximal side, the tilting of the 3-$CH_3$ out of plane upon saturation of the pyrrole $\beta$–$\beta$ bond would necessarily increase the distance between 3-$CH_3$ and any of the Ile 99 protons by ~2.8 Å compared to the native structure.

The determination of distance from NOEs in paramagnetic complexes is difficult unless either the selective relaxation rate of the detected peak can be determined, which yields $\sigma$ via the steady-state NOE and eq 1, or a time-dependent NOE can be measured for very short irradiation time, which directly yields $\sigma$ (Keller & Wüthrich, 1981; Ramaprasad et al., 1984). The rapid relaxation rates and minimal resolution in the two SMb complexes preclude executing useful truncated NOE experiments. However, both the steady-state NOE and the relaxation time for the detected peak could be determined for a pair of functional groups on Ile 99 (FG5) and on pyrrole B, namely, $\gamma$-$CH_3$ ($C_{16}$ or $A_{16}$) and 3-$CH_3$ ($C_{21}$ or $A_{21}$).

In the case of dominant paramagnetic contributions to relaxation, as in the case for the 3-$CH_3$ of SMbs ($T_1$ ~30–50 ms), the nonselective $T_1$ is essentialy the same as the selective $T_1$, and the 3-$CH_3$ $T_1$s in Table I may be used directly (Lecomte & La Mar, 1986). In met$S_C$MbCN, $T_1$ (3-$CH_3$) = 29 ± 1 ms, and saturation of the $\gamma$-$CH_3$ causes an ~−1.2 ± 0.3% intensity change in the 3-$CH_3$ signal.[5] This leads to $\sigma$ and 0.14 ± 0.05 $s^{-1}$, which yields $r$(3-$CH_3$–$\gamma$-$CH_3$) = 3.8 ± 0.3 Å. In met$S_A$MbCN, $T_1$ (3-$CH_3$) = 55 ± 3 ms, $\eta$($\gamma$-$CH_3$ → 3-$CH_3$)[5] = −1.1 ± 0.3%, which leads to $\sigma$ = 0.19 ± 0.04 $s^{-1}$ and $r$(3-$CH_3$–$\gamma$-$CH_3$) = 3.6 ± 0.3 Å.

The conserved orientation of Ile 99 (FG5) upon SMb formation is supported by the experimentally determined 5-$CH_3$ to $\delta$-$CH_3$ distance, which is 3.9 ± 0.1 Å in the native protein (Takano, 1977a,b). For met$S_A$MbCN, $\eta$(5-$CH_3$ → $\delta$-$CH_3$)[5] = −1.1 ± 0.2% and $T_1$ ($\delta$-$CH_3$) = 60 ± 6 ms, leading to $\sigma$ = 0.18 ± 0.02 $s^{-1}$ and $r$ = 3.6 ± 0.3 Å. In met$S_C$MbCN, $C_{12}$-($\delta$-$CH_3$) is incompletely resolved and a $T_1$ estimate is not

[3] NOEs to $C_{10}$ and $C_{27}$ are also observed, consistent with their assignment to resonances from nearby Phe CD1; confirmation of this assignment is in progress.

[4] Not resolved.

[5] To obtain $\eta_{ij}$, the change in intensity must be scaled to give the effect per irradiated proton.

possible, but a $T_1$ similar to $\delta$-$CH_3$ in met$S_A$MbCN is expected; the $\eta$(5-$CH_3$ → $\delta$-$CH_3$) ~−1.0 suggests that $r$(5-$CH_3$ → $\delta$-$CH_3$) is comparable in the two SMb complexes.

Thus, the two distances for $\delta$-$CH_3$ to 5-$CH_3$ and $\gamma$-$CH_3$ to 3-$CH_3$ determined by NOEs for the two SMb complexes dictate both that the orientation of Ile 99 (FG5) relative to the heme has not been significantly altered and that the distance between 3-$CH_3$ and the Ile 99 (FG5) $\gamma$-$CH_3$ is unchanged (or possibly decreased[6]) upon SMb formation. The latter result dictates that the 3-$CH_3$ in the saturated ring for both $S_C$Mb and $S_A$Mb must point toward the proximal side of the heme, and hence the chirality of $C_3$ is as shown in parts C and E of Figure 1 for $S_C$Mb and $S_A$Mb, respectively. The functionality of pyrrole B has been determined for $S_C$Mb (Chatfield et al., 1986c; Bondoc et al., 1986); that of $S_A$Mb must yet be elucidated, but the proposed episulfide (Berzofsky et al., 1972), if correct, would have the sulfur inserted from the *distal* side of the heme. The same absolute configuration about $C_3$ is consistent with the proposed conversion of the presumed episulfide of $S_A$Mb (**2**) to the thiolene ring of $S_C$Mb (**3**) (Chatfield et al., 1986c).

*Magnetic Properties.* The observation of upfield dipolar shifts for all protons of Ile 99 (FG5) for both met$S_C$MbCN and met$S_A$MbCN as previously found in native metMbCN (Ramaprasad et al., 1983, 1984) confirms our expectation that the magnetic properties are qualitatively similar, on the basis of the similar orbital ground state of the iron in the three complexes (Chatfield et al., 1988a,b). Moreover, the fact that the upfield pattern of dipolar shifts for the nonequivalent Ile 99 (FG5) protons are similar in met$S_C$MbCN, met$S_A$MbCN, and native metMbCN (Ramaprasad et al., 1984) (Table I) suggests not only that the magnetic axes have similar orientations but that the magnetic anisotropies vary in the order metMbCN > met$S_A$MbCN > met$S_C$MbCN. Earlier ESR data (Berzofsky et al., 1971) confirm a reduced spread of the three $g$ values of (presumably) met$S_A$MbCN relative to those of metMbCN. This difference in magnetic anistropy is supported by the pattern of $T_{1e}$s for the three complexes. Since both the efficiency of $T_{1e}$ relaxation and the magnitude of the $g$-tensor anisotropy (Byrn et al., 1983) can be related to the splitting of the Kramers doublet of the low-spin ferric ion (Palmer, 1979), long $T_{1e}$ (broad $^1$H lines) should parallel decreased magnetic anisotropy, as observed. A more quantitative description of both the electronic properties of the resulting met-cyano SMbs and the magnetic properties of the iron will require complete assignment of the heme resonances and surrounding amino acids. Such studies are in progress.

## Conclusions

(1) The spatial configuration of the substituents of pyrrole B of the alkaline terminal equilibration product SMb is found consistent with the thiolene ring previously proposed (Chatfield et al., 1986c, 1988b; Bondoc et al., 1986) for the reversibly extractable sulfhemin C.

(2) The chirality about $C_3$ in the initially formed SMb has the 3-methyl group pointed toward the proximal side of the heme with the heme orientation as described in the X-ray structure of native Mb. Hence, the attack of the sulfur atom is from the distal side. The exact functionality of this isomer is yet to be determined, but the present data are consistent with the proposed episulfide **2** (Berzofsky et al., 1972).

(3) The chirality about $C_3$ in the terminal alkaline equilibration product is the same as in the initially formed species; thus, the alkaline isomerization proceeds with retention of configuration about $C_3$.

(4) The observed $^1$H–$^1$H dipolar contacts between the heme and amino acids, as well as the amino acid dipolar shifts, indicate that both the local protein conformation and the qualitative magnetic properties of the heme iron are largely conserved upon the formation of sulfmyoglobin.

(5) The present NOE method suggests that it may be generally applicable toward determining the chirality of the saturated pyrrole of a chlorin if it can be uniquely incorporated into the pocket of a heme protein of known structure.

## Acknowledgments

We are indebted to V. Thanabal, J. S. de Ropp, and S. W. Unger for experimental assistance and to A. L. Balch and K. M. Smith for valuable discussions.

## References

Berzofsky, J. A., Peisach, J., & Blumberg, W. E. (1971) *J. Biol. Chem. 246*, 3367–3377.

Berzofsky, J. A., Peisach, J., & Horecker, B. L. (1972) *J. Biol. Chem. 247*, 3783–3791.

Bluhm, M. M., Bodo, G., Dintzis, H. M., & Kendrew, J. C. (1958) *Proc. R. Soc. London 246*, 369–389.

Bondoc, L. L., Chau, M.-H., Price, M. A., & Timkovich, R. (1986) *Biochemistry 25*, 8458–8466.

Byrn, M. P., Katz, B. A., Keder, N. L., Levan, K. R., Magurany, C. J., Miller, K. M., Pritt, J. W., & Strouse, C. E. (1983) *J. Am. Chem. Soc. 105*, 4916–4922.

Chatfield, M. J., La Mar, G. N., Balch, A. L., & Lecomte, J. T. J. (1986a) *Biochem. Biophys. Res. Commun. 135*, 309–315.

Chatfield, M. J., La Mar, G. N., Balch, A. L., Smith, K. M., Parish, D. W., & Le Page, T. J. (1986b) *FEBS Lett. 206*, 343–346.

Chatfield, M. J., La Mar, G. N., Lecomte, J. T. J., Balch, A. L., Smith, K. M., & Langry, K. C. (1986c) *J. Am. Chem. Soc. 108*, 7108–7110.

Chatfield, M. J., La Mar, G. N., & Kauten, R. J. (1987) *Biochemistry 26*, 6939–6950.

Chatfield, M. J., La Mar, G. N., Smith, K. M., Leung, H.-K., & Pandey, R. K. (1988a) *Biochemistry 27*, 1500–1507.

Chatfield, M. J., La Mar, G. N., Parker, W. O., Smith, K. M., Leung, H.-K., & Morris, I. K. (1988b) *J. Am. Chem. Soc. 110*, 6352–6358.

Cutnell, J. D., Bleich, H. E., & Glasel, J. A. (1976) *J. Magn. Reson. 21*, 43–46.

Cutnell, J. D., La Mar, G. N., & Kong, S. B. (1981) *J. Am. Chem. Soc. 103*, 5568–5573.

Emerson, S. D. (1988) Ph.D. Dissertation, University of California, Davis.

Jesson, J. P. (1973) in *NMR of Paramagnetic Molecules* (La Mar, G. N., Horrocks, W. D., Jr., & Holm, R. H., Eds.) pp 1–51, Academic Press, New York.

Keller, R. M., & Wüthrich, K. (1981) *Biol. Magn. Reson. 3*, 1–52.

Kretsinger, R. J., Watson, H. C., & Kendrew, J. C. (1968) *J. Mol. Biol. 31*, 305–314.

Kuriyan, J., Wilz, S., Karplus, M., & Petsko, G. A. (1986) *J. Mol. Biol. 192*, 133–154.

La Mar, G. N., & Budd, D. L. (1979) *Biochim. Biophys. Acta 581*, 201–209.

[6] This distance appears shorter than observed in the crystal structure as expected for a proximally tilted 3-$CH_3$; the outer limits of the uncertainties still place this distance at 2 Å smaller than would be seen for the alternate orientation.

La Mar, G. N., Emerson, S. D., Lecomte, J. T. J., Pande, U., Smith, K. M., Craig, G. W., & Kehres, L. A. (1986) *J. Am. Chem. Soc. 108*, 5568–5573.
Lecomte, J. T. J., & La Mar, G. N. (1986) *Eur. Biophys. J. 13*, 373–381.
Lecomte, J. T. J., Johnson, R. D., & La Mar, G. N. (1985) *Biochim. Biophys. Acta 829*, 268–274.
Levitt, M. H. (1982) *J. Magn. Reson. 48*, 234–264.
Levitt, M. H., & Freeman, R. (1979) *J. Magn. Reson. 33*, 473–476.
Miki, K., Ii, Y., Yukawa, M., Owatari, A., Hato, Y., Harada, S., Kai, Y., Kasai, N., Hata, Y., Tanaka, N., Kakudo, M., Katsubi, Y., Yoshida, Z., & Ogoshi, H. (1986) *J. Biochem. 100*, 209–276.
Noggle, J. H., & Shirmer, R. E. (1971) in *The Nuclear Overhauser Effect*, Academic Press, New York.
Palmer, G. (1979) in *The Porphyrins* (Dolphin, D., Ed.) Vol. 4B, pp 313–353, Academic Press, New York.
Ramaprasad, S., Johnson, R. D., & La Mar, G. N. (1983) *J. Am. Chem. Soc. 105*, 7205–7206.
Ramaprasad, S., Johnson, R. D., & La Mar, G. N. (1984) *J. Am. Chem. Soc. 106*, 5330–5335.
Schoenborn, B. P. (1967) *Nature (London) 207*, 28–30.
Schoenborn, B. P., Watson, H. C., & Kendrew, J. C. (1965) *Nature (London) 207*, 28–30.
Shulman, R. G., Glarum, S. H., & Karplus, M. (1971) *J. Mol. Biol. 57*, 93–115.
Swift, T. J. (1973) in *NMR of Paramagnetic Molecules* (La Mar, G. N., Horrocks, W. D., Jr., & Holm, R. H., Eds.) pp 58–83, Academic Press, New York.
Takano, T. (1977a) *J. Mol. Biol. 110*, 537–568.
Takano, T. (1977b) *J. Mol. Biol. 110*, 569–584.
Tilton, R. F., Jr., & Kuntz, J. D. Jr., (1982) *Biochemistry 21*, 6850–6857.
Tilton, R. F., Jr., Kuntz, J. D., Jr., & Petsko, G. A. (1984) *Biochemistry 23*, 2849–2952.
Unger, S. W., Jue, T., & La Mar, G. N. (1985) *J. Magn. Reson. 61*, 448–456.

# Classical Raman Spectroscopic Studies of NADH and $NAD^+$ Bound to Lactate Dehydrogenase by Difference Techniques†

Hua Deng,‡ Jie Zheng,‡ Donald Sloan,§ John Burgner,*,‖ and Robert Callender*,‡
*Physics and Chemistry Departments, City College of the City University of New York, New York, New York 10031, and Department of Biological Sciences, Purdue University, West Lafayette, Indiana 47907*
*Received July 25, 1988; Revised Manuscript Received September 16, 1988*

ABSTRACT: The binding of the coenzymes $NAD^+$ and NADH to lactate dehydrogenase causes significant changes in the Raman spectra of both of these molecules relative to spectra obtained in the absence of enzyme. The molecular motions of the bound adenine moiety of both $NAD^+$ and NADH as well as adenine containing analogues of these coenzymes produce Raman bands that are essentially identical, suggesting that the binding of adenine to the enzyme is the same regardless of the nicotinamide head-group nature. We also have observed that the molecular motions of the bound adenine moiety are different from both those obtained when it is in either water, various hydrophobic solvents, or various other solvent compositions. Protonation of the bound adenine ring at the 3-position is offered as a possible explanation. Significant shifts are observed in both the stretching frequency of the carboxamide carbonyl of $NAD^+$ and the rocking motion of the carboxamide $NH_2$ group of NADH. These shifts are probably caused by hydrogen bonding with the enzyme. The interaction energies of these hydrogen-bonding patterns are discussed. The aromatic nature of the nicotinamide moiety of $NAD^+$ appears to be unchanged upon binding. Pronounced changes in the Raman spectrum of the nicotinamide moiety of NADH are observed upon binding; some of these changes are understood and discussed. Finally, these results are compared to analogous results that were recently reported for liver alcohol dehydrogenase [Chen et al. (1987) *Biochemistry 26*, 4776–4784]. In general, the coenzyme binding properties are found to be quite similar, but not identical, for the two enzymes.

Recent studies of enzyme catalysis [cf. Jencks (1975, 1980, 1986), Schowen (1978), Wolfenden (1976, 1978), Cook et al. (1981), Somogyi et al. (1984), Stackhouse et al. (1985), and, Burgner et al. (1987)] have focused on the extent that enzymes use noncovalent interactions to facilitate the making and breaking of covalent bonds and to perform stereospecific reactions. The energy and origin of these noncovalent interactions have been difficult to assess experimentally until recently. Raman spectroscopy is known for its ability to provide detailed information concerning such molecular properties of molecules and the interactions between molecules such as those that occur when a substrate binds at the active site of an enzyme. This has been particularly true in resonance Raman experiments of prosthetic chromophores contained in the active sites of proteins as in, for example, visual pigments, heme proteins, and some enzymes [reviewed in Carey (1982) and in papers found in Spiro (1987)]. The resonantly enhanced Raman spectrum of the colored prosthetic group so dominates the protein classical Raman spectrum that it is easily detected

† This work was supported by Grants GM35183 (City College) and RCMI RRO3060 (City College) from the National Institutes of Health and Grant 8616216 from The National Science Foundation (Purdue University).
‡ Physics Department, City College of the City University of New York.
§ Chemistry Department, City College of the City University of New York.
‖ Department of Biological Sciences, Purdue University.

0006-2960/89/0428-1525$01.50/0 